Maximum Throughput Analysis in Hybrid Energy Harvesting Wireless Communication Systems Based on Martingale Theory

Hangyu Yan, Xuefen Chi, Wanting Yang, Zehui Xiong, *Senior Member, IEEE*, and Zhu Han, *Fellow, IEEE*

***Abstract*—In this article, based on martingale theory, we investigate the problem of maximum throughput in hybrid energy harvesting wireless communication systems (EH-WCSs) under energy storage and delay (or backlog) constraints. Specifically, the energy supply and data transmission of the hybrid EH-WCS are modeled as two queuing systems. For the first energy supply queueing system, we construct corresponding martingales for each type of energy harvesting (EH) process and the system's energy consumption process. Leveraging the multiplicativity of martingales, the stochastic characteristics of the hybrid EH process are described in the martingale domain. On this foundation, a closed-form expression for the energy depletion probability bound (EDPB) under various energy storage constraints is derived. In the second data transmission queueing system, to capture the impact of channel fading on the system's service, we map the arrival and service processes to the signal-to-noise ratio (SNR) domain and construct the corresponding martingales. A martingale parameter is proposed that connects the martingales of the arrival and service processes with the system's EDPB. Based on this, the closed-form expressions for the delay violation probability bound and backlog violation probability bound are derived. Utilizing these derived performance bounds, we address the maximum throughput optimization problems under the energy storage and delay (or backlog) constraints. Furthermore, we instantiate a scenario and provide guidance on the impact of resource allocation on maximum throughput through simulation and validation, offering insights for achieving green communication networks.**

***Index Terms*—Delay constraints, green communication, hybrid energy harvesting (EH), martingale theory, maximum throughput.**

Manuscript received 4 May 2024; revised 13 July 2024; accepted 10 August 2024. Date of publication 13 August 2024; date of current version 20 November 2024. This work was supported in part by the Natural Science Foundation of Jilin Province under Grant 20230101063JC, and in part by the China Scholarship Council CSC under Grant 202306170155. *(Corresponding author: Xuefen Chi.)*

Hangyu Yan and Xuefen Chi are with the Department of Communications Engineering, Jilin University, Changchun 130012, China (e-mail: yanhy21@mails.jlu.edu.cn; chixf@jlu.edu.cn).

Wanting Yang and Zehui Xiong are with the Information Systems Technology and Design Pillar, Singapore University of Technology and Design, Singapore (e-mail: wanting_yang@sutd.edu.sg; zehui_xiong@sutd.edu.sg).

Zhu Han is with the Department of Electrical and Computer Engineering, University of Houston, Houston, TX 77004 USA, and also with the Department of Computer Science and Engineering, Kyung Hee University, Seoul 446-701, South Korea (e-mail: hanzhu22@gmail.com).

Digital Object Identifier 10.1109/JIOT.2024.3443209

I. Introduction

IN RECENT years, the rapid increase in energy consumption (EC) of devices in wireless communication systems (WCSs) has raised concerns about environmental pollution and resource depletion [1]. Faced with this issue, energy harvesting (EH) technology is considered as an effective solution [2], [3], [4]. EH technology leverages renewable energy sources, such as solar, wind, or geothermal energy, to provide free and pollution-free energy supply to WCS, driving the industry toward a greener and more sustainable direction [5]. However, due to hardware limitations, environmental conditions, and weather factors, each type of energy harvested by devices at each moment is often stochastic and limited [6]. Meanwhile, existing Internet of Things systems and applications, such as industrial automation, remote healthcare, and intelligent transportation system, impose stringent Quality of Service (QoS) requirements on WCS in terms of latency, backlog and jitter [7], [8], [9]. These QoS requirements necessitate WCS to provide a substantial amount of stable and continuous energy supply. Therefore, hybrid EH has become an essential requirement for WCS.

The hybrid EH WCS (EH-WCS) is capable of simultaneously harvesting multiple types of energy from the environment to provide a substantial, diversified and sustainable energy supply for communication devices [10], [11], [12]. This advantage has spurred numerous researches on the maximum throughput of hybrid EH-WCS [13], [14], [15]. However, the existing literature primarily focuses on energy scheduling, power optimization, and EH methods, while often overlooking the impacts on system reliability, delay, and backlog [16]. System reliability refers to the probability that wireless devices operate normally when powered by a hybrid EH system. Therefore, there is a critical need to understand how to effectively utilize the limited energy and wireless transmission resources of hybrid EH-WCS to achieve maximum throughput while meeting the stringent QoS requirements of various services and applications [17]. Addressing this issue necessitates a precise performance analysis of hybrid EH-WCS, which involves tackling the following challenging problems.

1) The stochastic characteristics of different types of energy sources vary significantly. The combination of multiple energy types adds to the complexity and diversity of

the stochastic properties of the harvested hybrid energy. Accurately characterizing the stochastic nature of the hybrid EH process remains an unresolved issue.

2) In the hybrid EH-WCS, the hybrid EH at any given moment may exceed or fall short of the current EC. When hybrid EH surpasses EC, the surplus energy is wasted, while a shortfall in energy can cause system interruptions. To optimize energy efficiency, the system often includes a battery with limited capacity for storing surplus energy or compensating for EC during regular operations. Maximizing throughput of hybrid EH-WCS requires enhancing energy utilization efficiency. This entails a detailed analysis of the relationships between the energy depletion probability, battery capacity, the hybrid EH process, and EC process. In current literature, a robust method for this analysis is lacking.
3) The dynamic service of hybrid EH-WCS is simultaneously influenced by the hybrid EH process, battery capacity, energy depletion probability, and wireless channel fading. Current theoretical methods for analyzing delay and backlog primarily focus on the impact of channel fading, overlooking these additional variables. Additionally, these methods often suffer from loose estimation bounds due to the use of stochastic network calculus (SNC) [18]. Consequently, accurately assessing delay and backlog in hybrid EH-WCS remains a significant unresolved challenge.

Martingale theory is a powerful tool for analyzing stochastic processes [19]. It can transform various complex stochastic processes into martingales, endowing them with the properties of martingales, thereby making them easier to analyze. In light of these challenges, we propose a martingale-based framework to analyze the maximum throughput of hybrid EH-WCS. This system is modeled as a combination of an energy supply queue and a data transmission queue, as depicted in Fig. 1. In the data transmission queuing system, to capture the stochastic nature of the service process caused by wireless channel fading, the arrival process and the service process are mapped to the signal-to-noise ratio (SNR) domain through exponential transformations, avoiding the difficulty of obtaining the service distribution due to logarithmic operations. We employ martingale theory to analyze two queuing systems, thereby deriving the energy storage constraints, delay constraints, and backlog constraints of the hybrid EH-WCS. Based on these constraints, we further study the maximum throughput problem of the system. In summary, the main contributions of this article are shown below:

1) We construct corresponding martingales for each type of EH process and EC process. The stochastic properties of the hybrid EH process are described in the martingale domain by utilizing the multiplicativity of martingales. Then, based on queuing theory, we derive an upper bound on the cumulative energy deficit. Finally, leveraging the upper bound on the cumulative energy deficit and the constructed martingales, we derive a closed-form expression for the energy depletion probability bound (EDPB) under constraints of battery capacity, hybrid EH process, and EH process.
2) By leveraging martingale theory and Mellin transform, we construct martingales for both the arrival and service processes in the SNR domain. Next, a martingale parameter is introduced, which not only links the arrival and service processes but also takes into account the influence of EDPB on them. At last, with the constructed martingales, closed-form expressions for the delay violation probabilistic bound (DVPB) and backlog violation probabilistic bound (BVPB), subject to system EDPB constraints, are derived. Compared to existing SNC methods, the DVPB and BVPB derived by our method are accurate by several orders of magnitude.
3) Based on the derived performance bounds and the QoS requirements of different services, we formulate the maximum throughput optimization problem under energy storage and delay (or backlog) constraints. Subsequently, we consider a specific communication scenario for analysis and validation, providing insights into optimal resource allocation to achieve maximum throughput. This ensures that the system operates efficiently while meeting stringent QoS requirements.

This article is organized as follows. Section II introduces the related works. Section III introduces the system model and problem formulation. Section IV introduces the performance analysis model based on martingale theory. Section V conducts model instantiation. Numerical results and discussion are presented in Section VI, followed by conclusions in Section VII. The important notations used in this article are summarized in Table I.

II. Related Works

A. Throughput Analysis of EH-WCS

In recent years, some scholars have conducted research on the maximum throughput of EH-WCS. To overcome the drawbacks of ambient EH and wireless power transfer technologies while maximizing their benefits, Fu et al. [13] designed a hybrid energy offline scheduling scheme to enhance the point-to-point maximum throughput. Zhang et al. [14] proposed an offline power allocation algorithm and an online performance optimization scheme. These methods aim to maximize throughput in massive multiple inputs and multiple outputs systems with energy storage-constrained hybrid EH transmitters. However, in [13] and [14], the impact of delay or backlog on the maximum throughput was not addressed. Wang et al. [20] introduced a joint computation offloading and resource allocation algorithm based on the Lyapunov optimization technique. This algorithm optimized both communication and computation resources to enhance the network's maximum throughput for maritime edge computing nodes with EH capabilities. Li et al. [21] investigated the performance of each flow in a multichannel communication system with renewable EH and finite energy storage. They derived lower bounds on the maximum throughput for each flow under delay constraints and energy storage constraints, providing guidance for traffic admission control. Li et al. [22] investigated the maximum throughput performance of a multiuser wireless EH communication system under buffer constraints. They proposed an analysis of buffer overflow performance for bidirectional data

TABLE I
SUMMARY OF IMPORTANT NOTATIONS

Notation	Description
$\mathbb{E}[\cdot]$	Expectation operator
$\Pr(\cdot)$	Probability of event $(\cdot)$
$H_l(m,n)$	The cumulative energy harvesting process of energy l
$C(m,n)$	The cumulative energy consumption process of transmitter
$h_l(i)$	The number of the l-th type of energy blocks collected in the i-th time slot
$c(i)$	The number of energy blocks consumed in the i-th time slot
$A(m,n)$, $S(m,n)$, $D(m,n)$	Cumulative arrival, service and departure processes in the bit domain
$a(i)$, $s(i)$, $d(i)$	Instantaneous arrival, service and corresponding departure in the bit domain
$\widehat{A}(m,n)$, $\widehat{S}(m,n)$, $\widehat{D}(m,n)$	Cumulative arrival, service and departure processes in the SNR domain
$\widehat{a}(i)$, $\widehat{s}(i)$, $\widehat{d}(i)$	Instantaneous arrival, service and corresponding departure in the SNR domain
$W(n)$	The queuing delay at the n-th time slot
$Q(n)$	The backlog at the n-th time slot
$\Upsilon(n)$	The cumulative amount of energy deficits during the time interval $(0,n]$
$\mathcal{B}$	Battery capacity of the transmitter
w	The delay threshold
Ψ_b	The probability of energy depletion
Ψ_q	The queue overflow probability
Ψ_d	The delay violation probability
σ	The size of the queue buffer
τ_a	The throughput of the transmitter when there is no energy deficit
$\mathcal{M}_{\mathcal{Z}}(\vartheta)$	The Mellin transform of the variable $\mathcal{Z}$
$\mathrm{M}_{h_l}(m,n;\alpha)$	Martingales for the l-th energy harvesting process
$\mathrm{M}_c(m,n;\alpha)$	Martingales for energy consumption process
$\mathrm{M}_{\widehat{a}}(m,n;\vartheta)$	Martingales for arrival process
$\mathrm{M}_{\widehat{s}}(m,n;\vartheta)$	Martingales for service process

transmission and corresponding optimization schemes for power allocation and channel time allocation. Varan and Yener [23] proposed a directional water-filling algorithm to address the energy scheduling problem in EH communication networks and utilized forward induction to solve the data scheduling problem. They iteratively handle the maximum throughput problem with energy and delay constraints by alternately maximizing these two problems. However, the communication systems in [20], [21], [22], and [23] only consider single type of energy source.

B. Performance Analysis Based on SNC

SNC in the SNR domain is widely utilized to capture the stochastic service processes of wireless channels and conduct performance analysis regarding delay and backlog. Al-Zubaidy et al. [24] employed (min,×) SNC to capture the stochastic characteristics of Rayleigh fading channels and derived closed-form expressions for the BVPB and DVPB in WCS. Zhou et al. [25] proposed a predictable wireless resource scheduling scheme based on SNC theory and Lyapunov-guided proximal policy optimization algorithm. It addressed performance optimization challenges in industrial automation where real-time and time-sensitive traffic accessed wireless networks concurrently, ensuring a balance between delay control and throughput. Xiao et al. [26] and Zeng et al. [27] analyzed the impact of interference among users on delay based on the SNC. Subsequently, under delay constraints, they further investigated the power allocation problem for uplink and downlink nonorthogonal multiple access. Chen et al. [28] developed a model for a massive multiuser multiple-input multiple-output system supporting next-generation ultrareliable low-latency communication and analyzed the model's statistical QoS using SNC. Miao et al. [29] studied the worst-case end-to-end (E2E) performance of vehicular edge computing systems using SNC and derived a closed-form expression for the corresponding upper bound of E2E delay. Mei et al. [30] modeled a unmanned aerial vehicle (UAV) network integrating sensing and communication, and analyzed the network layer delay violations using SNC. Additionally, they proposed a delay minimization problem to reveal the tradeoff between sensing and communication under power allocation strategies. However, the existing SNC-based methods used in the aforementioned literature employ Boolean inequalities in the derivation process, which leads to the obtained performance bounds becoming loose. Additionally, the analysis of delay and backlog in existing methods does not consider the energy storage constraints of the hybrid EH-WCS.

C. Performance Analysis and Optimization Methods Based on Martingale Theory

Recently, martingale theory has proven to be superior in analyzing performance bounds within queueing systems [31]. Compared to the Boolean inequalities, the martingale-based Doob's inequalities can provide sharper stochastic bounds. Liu et al. [32] employed martingale theory to analyze the DVPB for uplink burst data transmission within vehicular federated learning scenarios. Then, they devised an optimization problem aimed at pinpointing the optimal adjustable parameter that maximizes the decay of global loss while adhering to an energy budget constraint. Picano and Fantacci [33] employed martingale theory to analyze the per-flow E2E delay bounds in a UAV-assisted multiaccess edge computing system, and proposed an efficient offloading strategy based on a matching algorithm. Yang et al. [34] applied a martingale-based resource estimation method to evaluate the minimum traffic required for transmitting specific video-on-demand streams under predefined QoS requirements. Considering the stochastic characteristics of fading channels, Yan et al. [35] constructed arrival and service martingales in the SNR domain, and subsequently derived a closed-form expression for the E2E-DVPB in multihop wireless links. Rezaee et al. [36] proposed an adaptive control scheme based on martingale theory to ensure the robustness of the vehicular network in scenarios where communication and vehicle radar data are randomly lost. However, when the service process of wireless channels is described using SNR and the impact of energy storage is considered, the martingale-based analysis methods for delay or backlog in [32], [33], [34], and [35] are no longer applicable. Additionally, there still lacks an effective martingale-based analysis method for EDPB.

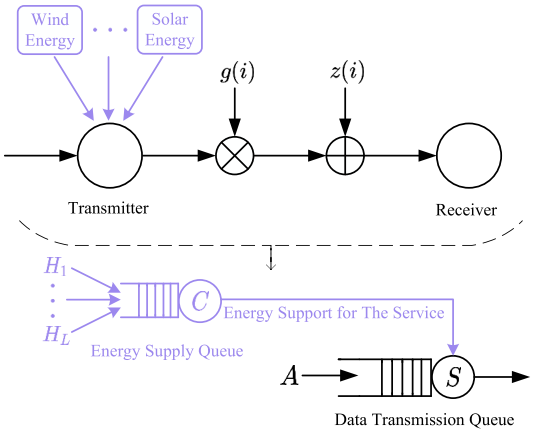

Fig. 1. Illustration of a hybrid EH-WCS.

III. System Model and Problem Formulation

A. System Model

We consider a WCS with hybrid EH capabilities, as shown in Fig. 1. The transmitter can harvest L types of energy from the surrounding environment, and each EH process is independent of the others. The harvested hybrid energy is consumed only for the system's data transmission. The system can be modeled as an energy supply queuing system together with a data transmission queuing system. In the energy supply queue system, the EH process is regarded as the input process of the queue, while the EC process is regarded as the service of the queue. We assume that the EH and EC processes are discrete over time and the energy exists in units of equal size energy blocks in the system [22]. Then, the cumulative EH process of energy l from time slots m to n can be expressed as $H_l(m,n) = \sum_{i=m+1}^{n} h_l(i), n > m \geq 0, l \in \mathcal{L} = \{1, 2, \ldots, L\}$, where $h_l(i)$ represents the number of the lth type of energy blocks collected in the ith time slot of the transmitter. Similarly, the cumulative EC process of transmitter can be represented as $C(m,n) = \sum_{i=m+1}^{n} c(i)$, where $c(i)$ is the number of energy blocks consumed in the ith time slot. It is essential to emphasize that the EH and the EC are mutually independent and both are stationary. The size of each energy block harvested or consumed is denoted as L_e (in unit of joules). Additionally, the transmitter contains a battery with a capacity of $\mathcal{B}$, and it is fully charged in the initial state. Moreover, the battery charging and discharging processes are ideal, with no losses. In a time slot, when the EH exceeds EC, the remaining energy is stored in the battery. If the battery is fully charged, the un-storable energy is discarded. If the amount of EH is less than the EC, an energy deficit occurs. In this case, the transmitter uses the energy stored in the battery to compensate for the current energy deficit. When the battery's energy is depleted, the system becomes inoperable. Based on the above conditions, the cumulative amount of energy deficits during the time interval $(0, n]$ can be characterized as

$$\Upsilon(n) = \max\left\{0, \Upsilon(n-1) + c(n) - \sum_{l=1}^{L} h_l(n)\right\}. \quad (1)$$

Due to the absence of energy deficit in the initial state of the hybrid EH-WCS, we define $\Upsilon(0) = 0$.

We model the wireless channel in the hybrid EH-WCS as a discrete time block fading channel [37]. The duration of each time slot is consistent with the time slot duration for EH and EC processes, and it is significantly shorter than the coherence time, defined as T_d. Let $x(i)$ represent the zero-mean and unit-power signal of the transmitter, and $y(i)$ denote the signal received at the receiver in the ith time slot, $i \geq 0$. The relationship between them can be expressed as

$$y(i) = \sqrt{\mathcal{P}} g(i) x(i) + z(i) \quad (2)$$

where $\mathcal{P}$ is the transmit power for the transmitter. It is determined by the EC process, and their relationship is expressed as $\mathcal{P} = c(i)L_e/T_d$. $g(i)$ is the complex channel coefficient between transmitter and receiver, which can be expressed as $g(i) = \sqrt{\hbar(i)}\zeta(i)$. $\hbar(i) = \ell^{-\kappa}$ is the path loss between the transmitter and receiver at the ith time slot, where ℓ is the distance between them and κ is the path loss exponent. In this scenario and within the considered time scale, $\hbar(i)$ remains constant. $\zeta(i)$ is the small-scale fading coefficients between the transmitter and receiver at the ith time slot, which is independent and identically distributed (i.i.d.) among different time slots and remains unchanged within a time slot. $z(i)$ is the additive white Gaussian noise at time slot i, which satisfies $\mathcal{CN}(0, \sigma^2)$. σ^2 denotes the noise power.

In alignment with [38], we assume that the receiver can obtain perfect channel state information (CSI), while the transmitter lacks or cannot acquire perfect CSI. Note that since the transmitter does not know the CSI of the wireless channel, it needs to send the signal with constant power. The instantaneous SNR at the receiver in the ith time slot can be expressed as $\gamma(i) = [(\mathcal{P}\hbar(i)|\zeta(i)|^2)/\sigma^2]$. Through the above analysis and modeling, it can be seen that the service of the wireless channel is influenced by the combination of channel fading, energy deficit and battery capacity. Therefore, we can derive the effective service process at the ith time slot, which is as follows:

$$s(i) = \begin{cases} T_d \cdot B \log_2(1+\gamma(i)), & \text{if } \Upsilon(i) \leq \mathcal{B} \\ 0, & \text{otherwise} \end{cases} \quad (3)$$

where B is the bandwidth. In the same way, the effective arrival process at the ith time slot can be expressed as

$$a(i) = \begin{cases} r_a(i), & \text{if } \Upsilon(i) \leq \mathcal{B} \\ 0, & \text{otherwise} \end{cases} \quad (4)$$

where $r_a(i)$ is the data transmission rate of the transmitter at the ith time slot when the energy is sufficient.

The cumulative arrival, service and departure processes can be expressed as $A(m,n) = \sum_{i=m+1}^{n} a(i)$, $S(m,n) = \sum_{i=m+1}^{n} s(i)$ and $D(m,n) = \sum_{i=m+1}^{n} d(i)$, where $a(i)$, $s(i)$, and $d(i)$ are the number of bits arrived, serviced, and departed in the ith time slot, respectively [27]. Similar to the EH and EC processes, the arrival and service processes are also independent and stationary stochastic processes. When the

hybrid EH-WCS is in a stable state, it needs to fulfil both of the following conditions:

$$\sum_{l=1}^{L}\mathbb{E}[h_l(i)] > \mathbb{E}[c(i)]$$
$$\mathbb{E}[a(i)] < \mathbb{E}[s(i)] \tag{5}$$

where $\mathbb{E}[\cdot]$ represents the expectation operator. Based on this, the delay of the hybrid EH-WCS at the nth time slot, defined as the number of time slots until the information data arriving at the nth time slot are successfully delivered, is expressed as [26]

$$W(n) = \inf\{w \geq 0 : A(0,n) \leq D(0,n+w)\} \tag{6}$$

where w is the delay threshold. The backlog of the hybrid EH-WCS at the nth time slot can be defined as

$$Q(n) = A(0,n) - D(0,n). \tag{7}$$

B. Problem Formulation

For the given hybrid EH-WCS, its energy storage constraint, denoted by $(\mathcal{B}, \Psi_b)$, can be defined as $\Pr(\Upsilon(n) > \mathcal{B}) \leq \Psi_b$. Ψ_b is the probability of energy depletion. The delay constraint and backlog constraint are defined as $\Pr(W(n) > w) \leq \Psi_d$ and $\Pr(Q(n) > \sigma) \leq \Psi_q$, which can be represented as (w, Ψ_d) and (σ, Ψ_q), respectively. Here, Ψ_d is the delay violation probability, Ψ_q is the queue overflow probability, and σ is the size of the queue buffer. Considering many delay-sensitive services, we formulate a maximum throughput optimization problem under delay and energy storage constraints as follows:

$$\begin{aligned} \max \quad & \tau_a \\ s.t. \quad & \Pr(\Upsilon(n) > \mathcal{B}) \leq \Psi_b \\ & \Pr(W(n) > w) \leq \Psi_d \end{aligned} \tag{8}$$

where τ_a represents the throughput of the transmitter when there is no energy deficit, and it can be expressed as $\tau_a = \mathbb{E}[a(i)]/(1-\Psi_b)$. Similarly, for applications with limited buffer size, we formulate the maximum throughput problem under energy storage and backlog constraints as follows:

$$\begin{aligned} \max \quad & \tau_a \\ s.t. \quad & \Pr(\Upsilon(n) > \mathcal{B}) \leq \Psi_b \\ & \Pr(Q(n) > \sigma) \leq \Psi_q. \end{aligned} \tag{9}$$

IV. Performance Analysis Model Based on Martingale Theory

In this section, we analyze the energy storage, delay, and backlog constraints of the hybrid EH-WCS based on martingale theory, and provide corresponding closed-form expressions.

A. Preliminaries

As shown in (3), due to the impact of the logarithmic operator, it is challenging to model the service process of the wireless channel in the bit domain. To deal with the above challenges, we resort to convert the analysis of the queue from the bit domain to the SNR domain by taking the exponential operation. The corresponding arrival, service and departure processes in the SNR domain can be expressed as $\widehat{A}(m,n) = e^{A(m,n)}$, $\widehat{S}(m,n) = e^{S(m,n)}$ and $\widehat{D}(m,n) = e^{D(m,n)}$, respectively. (min, $\times$) algebra plays a crucial role in linking the arrival, service, and departure processes of a system, forming the basis for performance analysis [24]. In the following definitions, we introduce the two most significant linear operations.

Definition 1 ([Min, $\times$] Convolution and Deconvolution): For any pair of bivariate processes $\widehat{X}(m,n)$ and $\widehat{Y}(m,n)$ in the SNR domain, one gets

$$\widehat{X} \otimes \widehat{Y}(m,n) \triangleq \inf_{0\leq m\leq u\leq n}\left\{\widehat{X}(m,u)\cdot\widehat{Y}(u,n)\right\} \tag{10}$$

and

$$\widehat{X} \oslash \widehat{Y}(m,n) \triangleq \sup_{u\leq m}\left\{\frac{\widehat{X}(u,n)}{\widehat{Y}(u,m)}\right\} \tag{11}$$

where "$\otimes$" and "$\oslash$" are (min, $\times$) convolution and deconvolution operators, respectively.

With the help of the (min, $\times$) convolution, the departure process in the SNR domain can be expressed as $\widehat{D}(0,n) \geq \widehat{A} \otimes \widehat{S}(0,n)$. Based on this, we can rewrite (7) and the queue backlog at the nth time slot can be re-expressed as

$$\begin{aligned} Q(n) &= \frac{\widehat{A}(0,n)}{\widehat{D}(0,n)} \\ &\leq \frac{\widehat{A}(0,n)}{\widehat{A}\otimes\widehat{S}(0,n)} \\ &= \frac{\widehat{A}(0,n)}{\inf_{0\leq m\leq n}\left\{\widehat{A}(0,m)\cdot\widehat{S}(m,n)\right\}} \\ &= \sup_{0\leq m\leq n}\left\{\frac{\widehat{A}(m,n)}{\widehat{S}(m,n)}\right\}. \end{aligned} \tag{12}$$

Similarly, the delay in (6) can be reformulated as

$$\begin{aligned} W(n) &= \inf\left\{w\geq 0 : \widehat{A}(0,n) \leq \widehat{D}(0,n+w)\right\} \\ &\leq \inf\left\{w\geq 0 : \sup_{0\leq m\leq n}\left\{\frac{\widehat{A}(0,n)}{\widehat{A}(0,m)\cdot\widehat{S}(m,n+w)}\right\} \leq 1\right\} \\ &\leq \inf\left\{w\geq 0 : \sup_{0\leq m\leq n}\left\{\frac{\widehat{A}(m,n)}{\widehat{S}(m,n+w)}\right\} \leq 1\right\}. \end{aligned} \tag{13}$$

The martingale theory is a powerful tool for the study of stochastic process. Let's review some crucial knowledge related to martingale theory by the following definition.

Definition 2 (Martingale Process): Let $\mathcal{F}_n$ is a filtration for the given probability space, where $\mathcal{F}_n \subseteq \mathcal{F}_{n+m}$, for $m,n \in \mathbb{N}$. If a discrete-time stochastic process $\{\mathcal{X}(n), n \geq 0\}$ is a discrete-time martingale process, it needs to satisfy [19]

$$\begin{aligned} &\mathbb{E}[|\mathcal{X}(n)|] < \infty \\ &\mathbb{E}[\mathcal{X}(n+1) \mid \mathcal{F}_n] = \mathcal{X}(n) \end{aligned} \tag{14}$$

where $\{\mathcal{X}(n); n \geq 0\}$ is $\mathcal{F}_n$ measurable. When the stochastic process $\{\mathcal{X}(n); n \geq 0\}$ is a super- or sub- martingale process, we can use $\leq$ or $\geq$ to replace the equal sign in (14). In the following context, the construction of martingales relies on the

Mellin transform [39]. Therefore, the definition is provided as follows.

Definition 3 (Mellin Transform): For a nonnegative stochastic variable $\mathcal{Z}$, its Mellin transform can be defined as

$$\mathcal{M}_{\mathcal{Z}}(\vartheta) = \mathbb{E}\left[\mathcal{Z}^{\vartheta-1}\right] \tag{15}$$

where ϑ is a free parameter.

B. Martingale Construction

Based on the knowledge and assumptions mentioned in the previous sections, we construct the corresponding martingales for the EH process, the EC process, the arrival process and the service process through the following lemmas.

Lemma 1 (Martingales for EH): Consider a hybrid EH-WCS that collects L types of energy from the surroundings. The accumulated EH process of any specific type of energy l can be represented as $H_l(m,n) = \sum_{i=m+1}^{n} h_l(i), n \geq m \geq 0, l \in \mathcal{L} = \{1,\ldots,L\}$. For every $\alpha > 0$, the following stochastic process:

$$\mathrm{M}_{h_l}(m,n;\alpha) = \mu_{h_l}(h_l(n))e^{\alpha\left((n-m)\Omega_{h_l} - H_l(m,n)\right)} \tag{16}$$

is a martingale process. $\mu_{h_l}(h_l(n))$ and Ω_{h_l}, which both implicitly depend on α, are used to construct a martingale process for the EH process. When the EH process is an i.i.d. stochastic process, $\mu_{h_l}(h_l(n)) = 1$ and $\Omega_{h_l} = -\ln(\mathbb{E}[e^{-\alpha h_l(i)}])/\alpha$. On the other hand, if the EH process is a Markov process with finite state space $\mathcal{S}_l = \{0,1,\ldots,N\}$, we can obtain the transition probability matrix $\mathbf{Q}$ of $h_l(i)$, where $\mathbf{Q}_{p,q} = \Pr(i+1 = q \mid i = p)$, and $p,q \in \mathcal{S}_l$. $h_l(i+1)$ and $h_l(i)$ represent the EH rates when in the q state and p state, respectively. The exponential transform of $\mathbf{Q}$ is defined as $\mathbf{Q}(-\alpha)$ which satisfies $\mathbf{Q}_{p,q}(-\alpha) = \Pr(i+1 = q \mid i = p)e^{-\alpha h_l(i+1)} = \mathbf{Q}_{p,q}e^{-\alpha h_l(i+1)}$. Thus, $\Omega_{h_l} \geq -\ln(sp(\mathbf{Q}(-\alpha)))/\alpha$ and $sp(\mathbf{Q}(-\alpha))$ is the spectral radius of the matrix $\mathbf{Q}(-\alpha)$. $\mu_{h_l}(h_l(n))$ is the parameter of the state corresponding to $h_l(n)$ in the right eigenvector associated with the spectral radius.

Proof: See Appendix A. ∎

Lemma 2 (Martingales for EC): Given a hybrid EH-WCS that expends energy to transmit data, its accumulated EC process can be denoted as $C(m,n) = \sum_{i=m+1}^{n} c(i), n \geq m \geq 0$. For every $\alpha > 0$, the following stochastic process:

$$\mathrm{M}_c(m,n;\alpha) = \mu_c(c(n))e^{\alpha(C(m,n)-(n-m)\Omega_c)} \tag{17}$$

is a martingale process. $\mu_c(c(n))$ and Ω_c, both of which implicitly depend on α, are employed to construct a martingale process for the EC process. When the EC process is an i.i.d. stochastic process, $\mu_c(c(n)) = 1$ and $\Omega_c = \ln(\mathbb{E}[e^{\alpha c(i)}])/\alpha$. In contrast, if the EC process is a Markov process with finite state space $\mathcal{S}_c = \{0,1,\ldots,M\}$, $\mathbf{P}$ is the transition probability matrix of $c(i)$. $\mathbf{P}(\alpha)$ is defined as its exponential column transformed matrix, which satisfies $\mathbf{P}_{p,q}(\alpha) = \Pr(i+1 = q \mid i = p)e^{\alpha c(i+1)} = \mathbf{P}_{p,q}e^{\alpha c(i+1)}, p,q \in \mathcal{S}_c$. Thus, $\Omega_c \geq \ln(sp(\mathbf{P}(\alpha)))/\alpha$ and $sp(\mathbf{P}(\alpha))$ is the spectral radius of the matrix $\mathbf{P}(\alpha)$. $\mu_c(c(n))$ is the parameter of the state corresponding to $c(n)$ in the right eigenvector associated with the spectral radius.

Proof: See Appendix A. ∎

Lemma 3 (Martingales for Arrival): For an i.i.d. arrival flow in the SNR domain, its accumulated arrival process can be expressed as $\widehat{A}(m,n) = \prod_{i=m+1}^{n} \widehat{a}(i), n \geq m \geq 0$, where $\widehat{a}(i)$ denotes the arrival at the ith time slot. The Mellin transform of $\widehat{a}(i)$ is $\mathcal{M}_{\widehat{a}(i)}(1+\vartheta) = \mathbb{E}[(\widehat{a}(i))^{\vartheta}]$. Furthermore, as $\widehat{a}(i)$ is i.i.d., $\mathcal{M}_{\widehat{a}}(1+\vartheta) = \mathcal{M}_{\widehat{a}(i)}(1+\vartheta)$ is achieved for all $\widehat{a}(i)$. Fix $\vartheta > 0$ and define $\Phi_{\widehat{a}}(1+\vartheta) = \mathcal{M}_{\widehat{a}}(1+\vartheta)^{1/\vartheta}$. Then, the stochastic process

$$\mathrm{M}_{\widehat{a}}(m,n;\vartheta) = \left(\frac{\widehat{A}(m,n)}{\Phi_{\widehat{a}}(1+\vartheta)^{n-m}}\right)^{\vartheta} \tag{18}$$

is a martingale process, and it is also a super-martingale.

Proof: See Appendix B. ∎

Lemma 4 (Martingales for Service): For the i.i.d. dynamic service provided by a wireless node in the SNR domain, its accumulated service process can be represented as $\widehat{S}(m,n) = \prod_{i=m+1}^{n} \widehat{s}(i), n \geq m \geq 0$, where $\widehat{s}(i)$ represents the service at the ith time slot. The Mellin transform of $\widehat{s}(i)$ is $\mathcal{M}_{\widehat{s}(i)}(1-\vartheta) = \mathbb{E}[(\widehat{s}(i))^{-\vartheta}]$. Due to $\widehat{s}(i)$ being i.i.d., we have $\mathcal{M}_{\widehat{s}}(1-\vartheta) = \mathcal{M}_{\widehat{s}(i)}(1-\vartheta)$ for all $\widehat{s}(i)$. Fix $\vartheta > 0$ and define $\Phi_{\widehat{s}}(1-\vartheta) = \mathcal{M}_{\widehat{s}}(1-\vartheta)^{-1/\vartheta}$. Then, the stochastic process

$$\mathrm{M}_{\widehat{s}}(m,n;\vartheta) = \left(\frac{\Phi_{\widehat{s}}(1-\vartheta)^{n-m}}{\widehat{S}(m,n)}\right)^{\vartheta} \tag{19}$$

is a martingale process, and it is also a super-martingale.

Proof: See Appendix B. ∎

C. Martingale-Based Performance Analysis

In this section, we analyze the performance bounds of the hybrid EH-WCS as depicted in Fig. 1 when it is in a stationary state. Based on (1), Lemmas 1 and 2, We employ martingale theory to establish the connection between the hybrid EH process, EC process, energy deficit, and battery capacity, and provide the following theorems.

Theorem 1 (EDPB): Consider a stable hybrid EH-WCS equipped with a battery of capacity $\mathcal{B}$. The system randomly collects L types of energy from the surrounding environment for data transmission. $\mathrm{M}_{h_l}(m,n;\alpha)$ and $\mathrm{M}_c(m,n;\alpha)$ are the martingale processes for the lth EH process and the system's EC process, $l \in \mathcal{L} = \{1,\ldots,L\}$. The EDPB can be expressed as

$$\Pr(\Upsilon(n) > \mathcal{B}) \leq \frac{\prod_{l=1}^{L}\mathbb{E}\left[\mu_{h_l}(h_l(n))\right]\mathbb{E}[\mu_c(c(n))]}{\Xi}e^{-\alpha^*\mathcal{B}} \tag{20}$$

where $\alpha^* = \sup\{\alpha > 0 : \Omega_c \leq \sum_{l=1}^{L}\Omega_{h_l}\}$ and $\Xi = \min_{c(n)>\sum_{l=1}^{L} h_l(n)}\{\prod_{l=1}^{L}\mu_{h_l}(h_l(n))\mu_c(c(n))\}$.

Proof: See Appendix C. ∎

Next, by utilizing (12) and (13) and Lemmas 3 and 4, we present the DVPB and BVPB for the hybrid EH-WCS, respectively.

Theorem 2 (DVPB): Given a stable hybrid EH-WCS equipped with a battery of capacity $\mathcal{B}$. Its energy storage constraint can be expressed as $(\mathcal{B}, \Psi_b)$. $\mathrm{M}_{\widehat{a}}(m,n;\vartheta)$ and $\mathrm{M}_{\widehat{s}}(m,n;\vartheta)$ are martingale processes of the arrival flow and the service provided by the wireless channel in the SNR

domain. Then, for any delay threshold $w \geq 0$, we have the DVPB as follows:

$$\Pr(W(n) > w) \leq \Phi_{\widehat{s}}\left(1-\vartheta^{\zeta}\right)^{-\vartheta^{\zeta} w} \tag{21}$$

where $\vartheta^{\zeta} = \sup\{\vartheta > 0 : \Phi_{\widehat{a}}(1+\vartheta) \leq \Phi_{\widehat{s}}(1-\vartheta)\}$. With the help of (4) and Lemma 3, $\Phi_{\widehat{a}}(1+\vartheta) = ((1-\Psi_b)\mathbb{E}[e^{\vartheta r_a(i)}] + \Psi_b)^{1/\vartheta}$ can be obtained. By the same way, with the help of (3) and Lemma 4, we can obtain $\Phi_{\widehat{s}}(1-\vartheta) = ((1-\Psi_b)\mathbb{E}[(1+\gamma(i))^{-[(BT_d\vartheta)/(\ln 2)]}] + \Psi_b)^{-1/\vartheta}$.

Proof: See Appendix D. ∎

Theorem 3 (BVPB): Given a stable hybrid EH-WCS equipped with a battery of capacity $\mathcal{B}$. Its energy storage constraint can be expressed as $(\mathcal{B}, \Psi_b)$. $\mathrm{M}_{\widehat{a}}(m,n;\vartheta)$ and $\mathrm{M}_{\widehat{s}}(m,n;\vartheta)$ are martingale processes of the arrival flow and the service provided by the wireless channel in the SNR domain. For any queue buffer size $\sigma \geq 0$, we have the BVPB as follows:

$$\Pr(Q(n) > \sigma) \leq e^{-\vartheta^{\zeta}\sigma} \tag{22}$$

where $\vartheta^{\zeta} = \sup\{\vartheta > 0 : \Phi_{\widehat{a}}(1+\vartheta) \leq \Phi_{\widehat{s}}(1-\vartheta)\}$. $\Phi_{\widehat{a}}(1+\vartheta)$ and $\Phi_{\widehat{s}}(1-\vartheta)$ as shown in Theorem 2.

Proof: See Appendix D. ∎

V. Model Instantiation

In this section, we first present specific constraints for maximizing throughput. Subsequently, we model the hybrid EH process, EC process, arrival process, and service process of the hybrid EH-WCS. Based on the conclusions derived in Section IV and the given model, we derive the necessary parameters and formulas required for maximum throughput.

A. Maximum Throughput Analysis

Based on the closed-form expressions derived for the EDPB and the DVPB in Section IV, the maximum throughput analysis problem in Section III [as in (8)] can be reformulated as

$$\begin{aligned}
\max \quad & \tau_a \\
s.t. \quad & \frac{\prod_{l=1}^{L}\mathbb{E}\left[\mu_{h_l}(h_l(n))\right]\mathbb{E}[\mu_c(c(n))]}{\Xi} e^{-\alpha^{*}\mathcal{B}} \leq \Psi_b \qquad (23a)\\
& \alpha^{*} = \sup\left\{\alpha > 0 : \Omega_c \leq \sum_{l=1}^{L}\Omega_{h_l}\right\} \qquad (23b)\\
& \Phi_{\widehat{s}}\left(1-\vartheta^{\zeta}\right)^{-\vartheta^{\zeta} w} \leq \Psi_d \qquad (23c)\\
& \vartheta^{\zeta} = \sup\{\vartheta > 0 : \Phi_{\widehat{a}}(1+\vartheta) \leq \Phi_{\widehat{s}}(1-\vartheta)\} \qquad (23d)
\end{aligned}$$

where (23a) and (23c) are energy storage and delay constraints, respectively. Equation (23b) and (23c) denote the stability conditions for the energy supply queue and the data transmission queue, respectively. Equation (23a) relates the L-type EH processes, EC process, and battery capacity to the given EDPB. Equation (23c) links the arrival process, the service process, the delay threshold, the DVPB and the EDPB. Similarly, by substituting the conditions in (23c), we can formulate the throughput maximization problem under energy and backlog constraints as follows:

$$\begin{aligned}
\max \quad & \tau_a \\
s.t. \quad & \text{(23a), (23b), (23d)} \\
& e^{-\vartheta^{\zeta}\sigma} \leq \Psi_q. \qquad (24)
\end{aligned}$$

B. Energy Harvesting and Energy Consumption Models

We assume that the hybrid energy harvested by the transmitter is composed of three different types of energy. In order to model the three different types of EH processes, we choose deterministic EH model, i.i.d. EH model and Markov process EH model, respectively. For the deterministic model, we adopt a constant rate EH model, where the energy blocks harvested in the ith time slot can be represented as

$$h_1(i) = \mathcal{R}_1. \tag{25}$$

Then we can take $\mathbb{E}[\mu_{h_1}(h_l(n))] = 1$ and $\Omega_{h_1} = \mathcal{R}_1$.

For the i.i.d. stochastic EH model, we consider it following a Poisson distribution, as illustrated below [40]:

$$\Pr(h_2(i) = \mathcal{R}_2) = \frac{\lambda^{\mathcal{R}_2} e^{-\lambda}}{\mathcal{R}_2!}, \mathcal{R}_2 = 0, 1, 2, \ldots \tag{26}$$

where $\Pr(h_2(i) = \mathcal{R}_2)$ denotes the probability that $\mathcal{R}_2$ energy blocks are harvested in the ith time slot, and λ denotes the mean of the harvested energy blocks. Then, we can get the $\mathbb{E}[\mu_{h_2}(h_2(n))] = 1$ and $\Omega_{h_2} = -([\lambda(e^{-\alpha}-1)]/\alpha)$.

The last type of EH process is modeled as a Markov modulated on-off process with a state space $\{0, 1\}$. When in state 1, the system is on state and it harvests $\mathcal{R}_3$ energy blocks; when in state 0, the system is off state and it does not harvest any energy [41]. p and q represent the transition probabilities between the two states, and the state changes at each time slot. We can obtain the transition probability matrix as

$$\mathbf{Q} = \begin{bmatrix} 1-p & p \\ q & 1-q \end{bmatrix}. \tag{27}$$

The stationary distribution of $h_3(i)$ can be given as

$$\begin{aligned}
\pi_0 &= \Pr(h_3(i) = 0) = \frac{q}{p+q} \\
\pi_1 &= \Pr(h_3(i) = \mathcal{R}_3) = \frac{p}{p+q}. \qquad (28)
\end{aligned}$$

Further, the exponential transition matrix of the matrix $\mathbf{Q}$ can be expressed as

$$\mathbf{Q}(-\alpha) = \begin{bmatrix} 1-p & pe^{-\alpha\mathcal{R}_3} \\ q & (1-q)^{-\alpha\mathcal{R}_3} \end{bmatrix} \tag{29}$$

where $\alpha > 0$. Its spectral radius can be expressed as $sp(\mathbf{Q}(-\alpha))$, and the corresponding right eigenvector is $V = [\mu_{h_3}(0), \mu_{h_3}(\mathcal{R}_3)]^T$. We can obtain $\Omega_{h_3} \geq -\ln(sp(\mathbf{Q}(-\alpha)))/\alpha$ and $\mathbb{E}[\mu_{h_3}(h_3(n))] = \pi_0 \times \mu_{h_3}(0) + \pi_1 \times \mu_{h_3}(\mathcal{R}_3)$.

According to the description of the system model, the receiver knows perfect CSI and the transmitter adopts constant power for transmission. Therefore, the EC process is modeled as a constant rate model as follows:

$$c(i) = \mathcal{R}_c. \tag{30}$$

Then, we can get $\mathbb{E}[\mu_c(c(n))] = 1$ and $\Omega_c = \mathcal{R}_c$. It should be noted that for the aforementioned EH and EC models, their parameter selection needs to satisfy the requirements specified in (5).

C. Arrival and Service Models

According to (3) and (4), the modeling of the arrival process and service process needs to consider not only the original distribution of the arrival traffic generated by the transmitting node and the service of the receiving node but also the impact of system downtime due to the lack of energy. We model the arrival process of traffic as a Bernoulli process. Considering the probability of energy depletion, the actual arrival process can be represented as

$$a(i) = \begin{cases} \mathcal{R}_a, & p_a(1-\Psi_b) \\ 0, & (1-p_a)+p_a\Psi_b \end{cases} \tag{31}$$

where $\mathcal{R}_a$ is the number of bits of arrival traffic and p_a is the probability of traffic arrival. According to Lemma 3, we can calculate

$$\Phi_{\widehat{a}}(1+\vartheta) = \left(1-p_a+p_a\Psi_b+p_a(1-\Psi_b)e^{\vartheta\mathcal{R}_a}\right)^{1/\vartheta}. \tag{32}$$

The Nakagami-m fading model often exhibits excellent fitting characteristics with measurement data in numerous multipath propagation environments, making it widely utilized in the modeling and analysis of wireless channels [42]. Therefore, we model small-scale fading as the Nakagami-m distribution. For a given m, the probability density function (PDF) of $\xi = |\zeta(i)|^2$ is as follows:

$$f(\xi) = \frac{m^m}{\Gamma(m)}\xi^{m-1}e^{-m\xi}, m \geq 0.5 \tag{33}$$

where m is Nakagami parameter. $\Gamma(x) = \int_0^\infty x^{t-1}e^{-t}dt$ is the Gamma function. Leveraging (3) and Lemma 4, we can derive the Mellin transform of the wireless channel's service process as follows:

$$\begin{aligned}
\mathcal{M}_{\widehat{s}}(1-\vartheta) &\overset{a}{=} (1-\Psi_b)\mathbb{E}\left[\left(1+\frac{\mathcal{P}\ell^{-\kappa}\xi}{\sigma^2}\right)^{-\frac{BT_d\vartheta}{\ln 2}}\right]+\Psi_b \\
&\overset{b}{=} \int_0^\infty (1-\Psi_b)\left(1+\frac{\mathcal{P}\ell^{-\kappa}\xi}{\sigma^2}\right)^{-\frac{BT_d\vartheta}{\ln 2}} \\
&\quad \times \frac{m^m}{\Gamma(m)}\xi^{m-1}e^{-m\xi}d\xi+\Psi_b \\
&\overset{c}{=} \frac{1-\Psi_b}{\Gamma(m)}\left(\frac{m\sigma^2}{\mathcal{P}\ell^{-\kappa}}\right)^m \\
&\quad \times \int_0^\infty (1+u)^{-\frac{BT_d\vartheta}{\ln 2}}u^{m-1}e^{-\frac{m\sigma^2}{\mathcal{P}\ell^{-\kappa}}u}du+\Psi_b \\
&\overset{d}{=} (1-\Psi_b)\left(\frac{m\sigma^2}{\mathcal{P}\ell^{-\kappa}}\right)^m \\
&\quad \times U\left(m, m+1-\frac{BT_d\vartheta}{\ln 2}, \frac{m\sigma^2}{\mathcal{P}\ell^{-\kappa}}\right)+\Psi_b
\end{aligned} \tag{34}$$

where step c is obtained by use $u = [(\mathcal{P}\ell^{-\kappa}\xi)/\sigma^2]$. $U(a,b,z) = (1/[\Gamma(a)])\int_0^\infty x^{a-1}(1+u)^{b-a-1}e^{-zu}du$ is the confluent hypergeometric Kummer U-function [43]. Hence, we can get

$$\begin{aligned}
\Phi_{\widehat{s}}(1-\vartheta) = \Bigg((1-\Psi_b)\left(\frac{m\sigma^2}{\mathcal{P}\ell^{-\kappa}}\right)^m \\
\times U\left(m, m+1-\frac{BT_d\vartheta}{\ln 2}, \frac{m\sigma^2}{\mathcal{P}\ell^{-\kappa}}\right)+\Psi_b\Bigg)^{-1/\vartheta}.
\end{aligned} \tag{35}$$

By substituting the derived parameters of the hybrid EH process, EC process, arrival process, and service process into (23) and (24), we can solve the maximum throughput problem under the relevant constraints.

TABLE II
SIMULATION PARAMETERS

Parameter	Value
The duration of a time slot T_d	1 ms
The size of each energy block L_e	1 mJ
The size of the arrival traffic packet	1 Kbits
Distance between transmitter and receiver ℓ	700 m
Path loss exponent κ	4
Noise power spectral density	-174 dBm/Hz
Bandwidth B	2 MHz

VI. Numerical Results and Discussion

In this section, we first validate the accuracy of the derived performance bounds through numerical simulations. Building upon this foundation, we further discuss the impact of various parameters on the maximum throughput of the hybrid EH-WCS under energy storage and delay (or backlog) constraints. Each simulation generates 10^8 simulated data following specified distributions using Monte Carlo methods, and we conduct 100 simulations. Some of the simulation parameters are shown in Table II.

A. Comparison of Theoretical Values and Simulation Results

In Fig. 2, we validate the accuracy and universality of the derived (20) in estimating the system EDPB. Considering the influence of different hybrid EH models, we set up Fig. 2(a) and (b) accordingly. In Fig. 2(a), the hybrid EH process is composed of a mixture of the Poisson EH process and the Markov EH process. In Fig. 2(b), the hybrid EH process comprises a combination of the constant rate EH process, the Poisson EH process, and the Markov EH process. To further verify the impact of changes in model parameters on the estimated EDPB accuracy, we set multiple groups of different EH and EC parameters for comparison in Fig. 2(a) and (b). It can be observed that the EDPB estimated by (20) closely matches the simulation results and exhibits the same decay trend under different types and parameters of models. Furthermore, it can be obtained that the EDPB exhibit a negative correlation with the hybrid EH process and battery capacity, while showing a positive correlation with the EC process. It is noteworthy that changing any single parameter alone has a limited impact on EDPB. To improve the system's EDPB, it is necessary to consider the combined effect of multiple parameters. Leveraging this relationship can optimize the energy supply of hybrid EH-WCS.

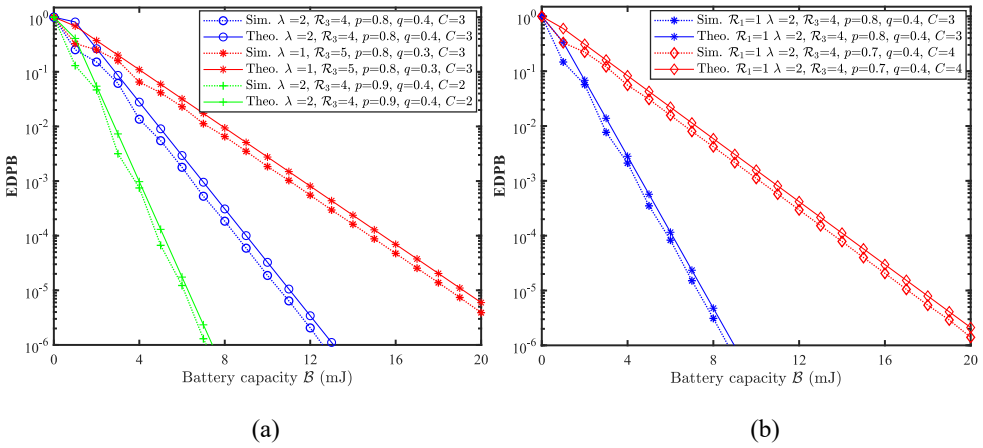

Fig. 2. Theoretical and simulation EDPB versus battery capacity under different hybrid EH processes. (a) Hybrid EH processes consist of two types of EH processes. (b) Hybrid EH processes consist of three types of EH processes.

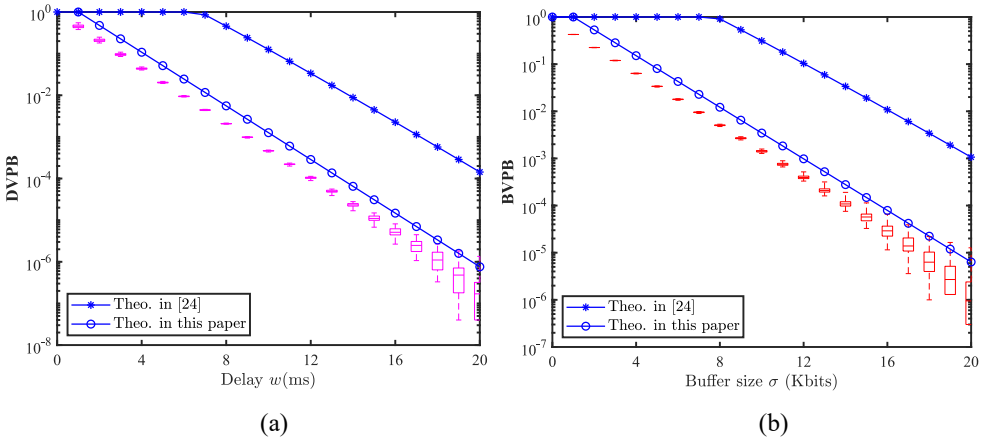

Fig. 3. Comparison of simulation results with theoretical values. (a) DVPB versus delay. (b) BVPB versus buffer size. The box plots are used to represent the simulation results.

In Fig. 3, we verify the accuracy of the DVPB estimated based on (21) and the BVPB estimated based on (22), respectively. In the simulation experiments, the arrival parameters are set to $\mathcal{R}_a = 3$ packets/slot, $p_a = 0.7$. For the service parameters, we assume that the consumed energy results in an average SNR of $\bar{\gamma} = 3$ dB at the receiver, with a parameter of $m = 2$ for the channel small-scale fading. The EDPB is set to $\Psi_b = 0.001$. The estimated DVPB, and the BVPB are compared with the simulation results and [24], respectively. The analysis method in [24] is widely used in delay analysis and backlog analysis of wireless channels. As can be seen in Fig. 3(a) and (b), the theoretical bounds estimated by our derived equations more precisely capture the impact of changes in delay thresholds and queue sizes on the DVPB and BVPB. They closely align with the simulation results and are significantly more precise than the theoretical values obtained using the analysis method in [24]. Therefore, compared to the approach in [24], our derived equations can achieve the same QoS requirements with less resource consumption.

B. Comparing the Effect of Different Parameters on Maximum Throughput

In this section, we set some default parameters as follows: $\Psi_b = 0.001$, $\Psi_d = 0.00001$, $\Psi_q = 0.00001$, $p_a = 0.8$, $\mathcal{B} =$ 10 mJ, $\mathcal{R}_1 = 1$, $\lambda = 2$, $\mathcal{R}_3 = 4$, $p = 0.8$, and $q = 0.4$. When the impact of the parameter on the maximum throughput has not been verified, default values are used in the simulation.

Fig. 4(a) and (b) demonstrate the impact of various parameters in hybrid EH processes on maximum throughput under (23) and (24), respectively. In Fig. 4(a), it can be observed that with the continuous increase of the delay w, the maximum throughput first increases rapidly, then increases slowly, and finally stabilizes. This indicates that in hybrid EH-WCS, appropriately relaxing the delay constraints can significantly enhance the system throughput. However, beyond a certain delay threshold, the effectiveness diminishes significantly. Comparing the red and green lines in the figure, it can be seen that for the same type of hybrid EH process, increasing the EH rate can improve the maximum throughput. Furthermore, by comparing the magenta, blue, and green lines, we can observe that although the means of the three hybrid EH processes are the same, the resulting maximum throughput differs. This is attributed to the differences in the mean of the Poisson EH process and the value of the constant rate EH process in each hybrid EH process. As the mean of the Poisson EH process decreases and the value of the constant rate EH process increases in the hybrid EH process, the maximum throughput increases. Compared to the constant rate EH

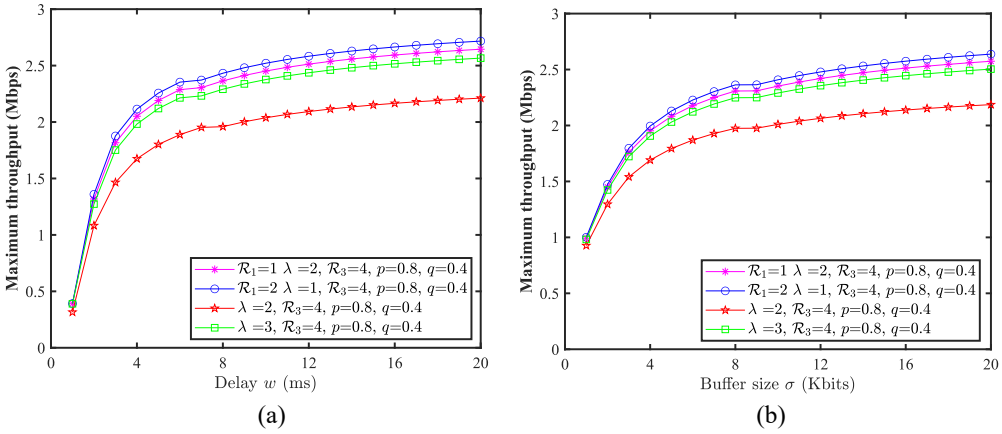

Fig. 4. Impact of various hybrid EH processes on maximum throughput. (a) Results under energy storage and delay constraints. (b) Results under energy storage and backlog constraints.

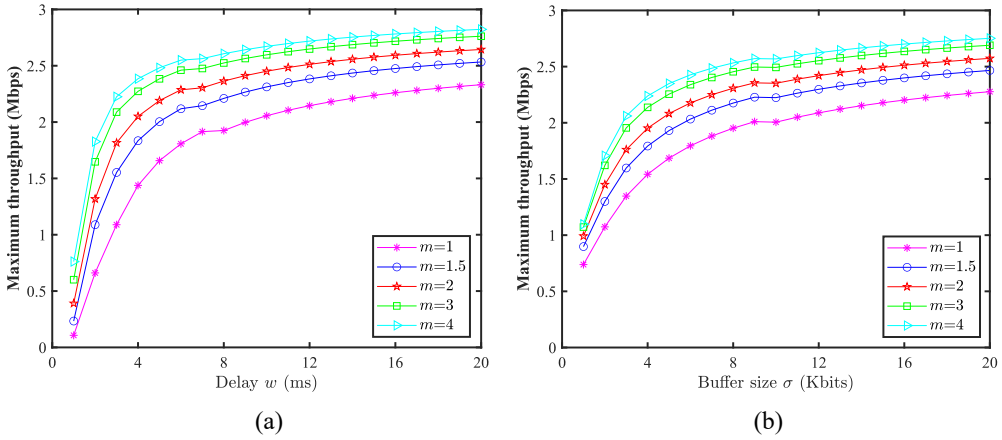

Fig. 5. Impact of various m on the maximum throughput. (a) Results under energy storage and delay constraints. (b) Results under energy storage and backlog constraints.

process, the Poisson EH process exhibits higher uncertainty. This results in an increased probability of not meeting or exceeding the EC in each time slot of the corresponding hybrid EH process. Consequently, the efficiency of harvested energy utilization declines, diminishing the system's service capacity and ultimately reducing the maximum throughput. Similarly, the same results are obtained in Fig. 4(b).

In Fig. 5(a) and (b), we present the influence of different channel parameters m on the maximum throughput under constraints of (23) and (24), respectively. When m increases, the fading of the wireless channel becomes smoother, and multipath effects weaken, resulting in better channel conditions. From the figure, it can be observed that as m increases, the maximum throughput also increases. This indicates that a more stable wireless channel can provide greater service capacity to meet higher throughput demands. However, as m increases, the rate of growth in maximum throughput begins to slow down. This also illustrates that the improvement in wireless channel state has limitations on the maximum throughput enhancement.

Fig. 6(a) and (b) display the impact of various energy depletion probabilities Ψ_b on the maximum throughput under constraints of (23) and (24), respectively. It can be seen from the figure that for applications with relatively loose delay or buffer size constraints, setting a looser Ψ_b can enhance the system's maximum throughput. In contrast, for applications with strict delay or buffer size constraints, a smaller Ψ_b is required to maximize throughput. Additionally, for applications with stringent delay or buffer constraints, when Ψ_b exceeds 10^{-2}, the improvement in maximum throughput becomes negligible. Therefore, for such applications, designing an appropriate Ψ_b is sufficient, and there is no need to expend significant resources to establish a very strict Ψ_b.

In Fig. 7(a) and (b), we exhibit the impact of battery capacity on maximum throughput under constraints of (23) and (24), respectively. As depicted in Fig. 7, when the battery capacity is low, relaxing the constraints on delay or buffer size does not effectively enhance the maximum throughput. This is because that the low-battery capacity leads to a considerable amount of harvested energy being wasted, which cannot contribute effectively to enhancing the service capacity of the wireless channel. As a result, the maximum throughput cannot increase effectively. Additionally, it can be observed that the maximum throughput increases rapidly at first, then increases slowly as the battery capacity increases, eventually leveling off. This indicates that as the battery capacity increases, its

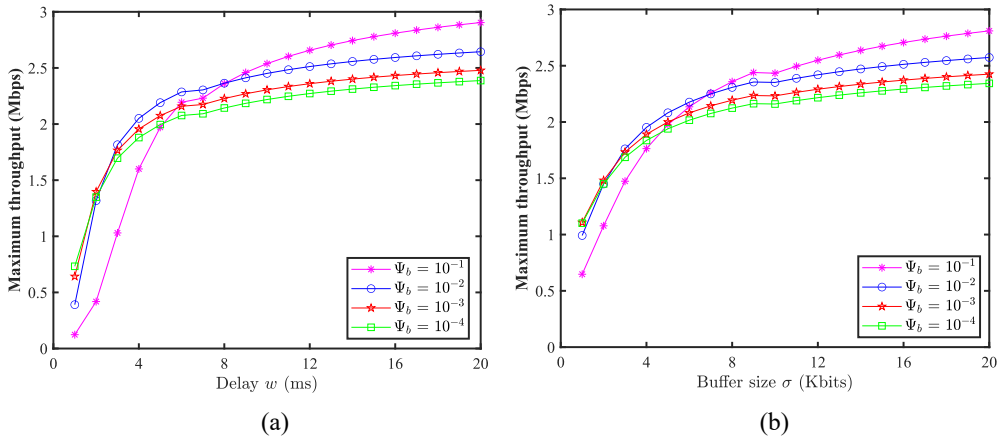

Fig. 6. Impact of different EDPB on maximum throughput. (a) Results under energy storage and delay constraints. (b) Results under energy storage and backlog constraints.

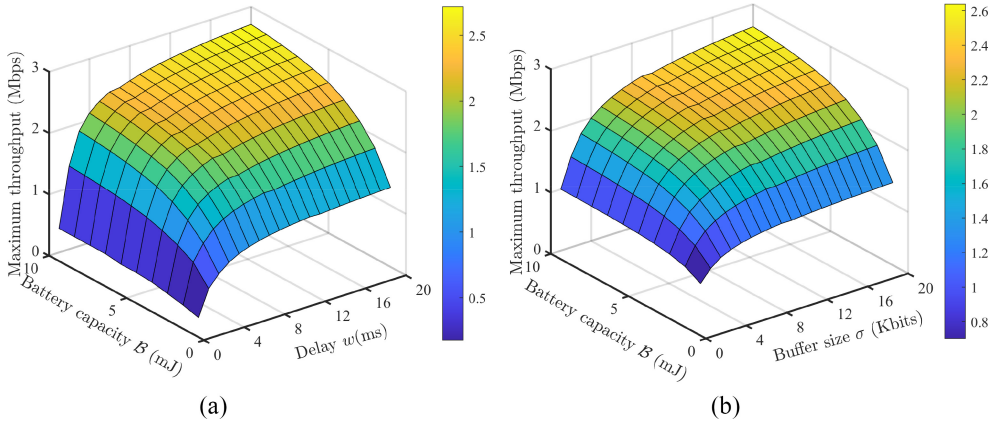

Fig. 7. Impact of various battery capacities on maximum throughput. (a) Results under energy storage and delay constraints. (b) Results under energy storage and backlog constraints.

impact on the maximum throughput gradually diminishes, and there exists a battery capacity threshold beyond which the maximum throughput tends to stabilize around a certain value.

In Figs. 4–7, it can be observed that when w or σ is 0, there are no value for throughput. We explain this issue using w as an example. When w is 0, in (23c), the left side of the inequality is always equal to 1. However, Ψ_d is a value much smaller than 1. Therefore, the above constraint is not satisfied, and the optimization problem has no solution at 0. Similarly, when σ is set to 0, the same result occurs.

VII. Conclusion

In this article, we developed corresponding queuing systems for both energy supply and data transmission within a hybrid EH-WCS, and conducted performance analyses of these queues using martingale theory. Based on the derived closed-form expression for EDPB, we precisely analyzed the relationships among the hybrid EH process, the EC process, battery capacity, and energy depletion probability. The closed-form expressions for DVPB and BVPB not only considered the stochastic characteristics of the fading channel and the impact of EDPB but also surpassed the accuracy of existing SNC methods by several orders of magnitude. Given these derived performance bounds, we addressed the problem of maximum throughput under constraints of energy storage and delay (or backlog). Through analysis in a specific application scenario, we examined how variations in resource parameters affected the system's maximum throughput. Simulation results indicated that when the mean of the hybrid EH process remained constant, an increase in its uncertainty led to a reduction in energy efficiency, which in turn caused a decrease in maximum throughput. Furthermore, resource parameters, such as battery capacity, channel fading coefficient, delay, and backlog, all show a positive correlation with maximum throughput. However, it should be noted that the increase of a single parameter had limited effects on enhancing maximum throughput. Significant improvements in maximum throughput required the combined action of these parameters.

Appendix A
Proof of Lemmas 1 and 2

Based on the definition of martingale as shown in Definition 2, we aim to prove that (16) is a martingale process. For the EH process, it is clear that the first condition is satisfied and it has a finite expectation. When the EH process is an i.i.d. stochastic process, let $\mu_{h_l}(h_l(n)) = 1$ and $\Omega_{h_l} =$

$-\ln(\mathbb{E}[e^{-\alpha h_l(i)}])/\alpha$. Then, we can derive

$$\begin{aligned}&\mathbb{E}\left[\mathrm{M}_{h_l}(m,n+1;\alpha)\mid h_l(1),h_l(2),\ldots,h_l(n)\right]\\&=e^{\alpha\left((n-m)\Omega_{h_l}-H_l(m,n)\right)}\mathbb{E}\left[e^{-\alpha h_l(n+1)}\right]e^{\alpha\Omega_{h_l}}\\&=\mathrm{M}_{h_l}(m,n;\alpha).\end{aligned}\tag{36}$$

When the EH process is a Markov process, we can derive

$$\begin{aligned}&\mathbb{E}\left[\mathrm{M}_{h_l}(m,n+1;\alpha)\mid h_l(1),h_l(2),\ldots,h_l(n)\right]\\&\overset{a}{=}e^{\alpha\left((n-m)\Omega_{h_l}-H_l(m,n)\right)}\\&\qquad\times\mathbb{E}\left[\mu_{h_l}(h_l(n+1))e^{-\alpha h_l(n+1)}\mid h_l(n)\right]e^{\alpha\Omega_{h_l}}\\&\overset{b}{=}e^{\alpha\left((n-m)\Omega_{h_l}-H_l(m,n)\right)}\left(\mathbf{Q}(-\alpha)\mu_{h_l}(h_l(n))\right)e^{\alpha\Omega_{h_l}}\\&\overset{c}{=}\mu_{h_l}(h_l(n))e^{\alpha\left((n-m)\Omega_{h_l}-H_l(m,n)\right)}sp(\mathbf{Q}(-\alpha))e^{\alpha\Omega_{h_l}}\\&\overset{d}{\leq}\mathrm{M}_{h_l}(m,n;\alpha)\end{aligned}\tag{37}$$

where the Perron–Frobenius theorem is used in step c. The matrix $\mathbf{Q}(-\alpha)$ is as described in Lemma 1, $\Omega_{h_l}\geq-\ln(sp(\mathbf{Q}(-\alpha)))/\alpha$ and $sp(\mathbf{Q}(-\alpha))$ is the spectral radius of the matrix $\mathbf{Q}(-\alpha)$.

The proof for the EC process is similar to that for the EH process. In practical applications, the expectation of the EC process is both existent and finite, and thus, we have $\mathbb{E}[c(i)]<\infty, i\geq 0$. When the EC process is an i.i.d. stochastic process, let $\mu_c(c(m))=1$ and $\Omega_c=\ln(\mathbb{E}[e^{\alpha c(i)}])/\alpha$. Then, we can get

$$\begin{aligned}&\mathbb{E}[\mathrm{M}_c(m,n+1;\alpha)\mid c(1),c(2),\ldots,c(n)]\\&=e^{\alpha(C(m,n)-(n-m)\Omega_c)}\mathbb{E}\left[e^{\alpha c(n+1)}\right]e^{-\alpha\Omega_c}\\&=\mathrm{M}_{h_l}(m,n;\alpha).\end{aligned}\tag{38}$$

In contrast, if the EC process is a Markov process, we can derive

$$\begin{aligned}&\mathbb{E}[\mathrm{M}_c(m,n+1;\alpha)\mid c(1),c(2),\ldots,c(n)]\\&=e^{\alpha(C(m,n)-(n-m)\Omega_c)}\\&\qquad\times\mathbb{E}\left[\mu_c(c(n+1))e^{\alpha c(n+1)}\mid c(n)\right]e^{-\alpha\Omega_c}\\&=e^{\alpha(C(m,n)-(n-m)\Omega_c)}(\mathbf{P}(\alpha)\mu_c(c(n)))e^{-\alpha\Omega_c}\\&=\mu_c(c(n))e^{\alpha(C(m,n)-(n-m)\Omega_c)}sp(\mathbf{P}(\alpha))e^{-\alpha\Omega_c}\\&\leq\mathrm{M}_c(m,n;\alpha)\end{aligned}\tag{39}$$

where the matrix $\mathbf{P}(\alpha)$ is as described in Lemma 2, $\Omega_c\geq\ln(sp(\mathbf{P}(\alpha)))/\alpha$ and $sp(\mathbf{P}(\alpha))$ is the spectral radius of the matrix $\mathbf{P}(\alpha)$.

Appendix B
Proof of Lemmas 3 and 4

In order to prove that $\mathrm{M}_{\widehat{a}}(m,n;,\vartheta)$ is a martingale process, it needs to satisfy the definition of martingale. The expectation for arrival flow is limited, and therefore, the remaining condition needs to be satisfied. We can derive

$$\begin{aligned}&\mathbb{E}[\mathrm{M}_{\widehat{a}}(m,n+1;\vartheta)\mid\widehat{a}(1),\widehat{a}(2),\ldots,\widehat{a}(n)]\\&\overset{a}{=}\mathbb{E}\left[\left(\frac{\widehat{A}(m,n)}{\Phi_{\widehat{a}}(1+\vartheta)^{n-m}}\right)^{\vartheta}\times\left(\frac{\widehat{a}(n+1)}{\Phi_{\widehat{a}}(1+\vartheta)}\right)^{\vartheta}\right]\\&\overset{b}{=}\left(\frac{\widehat{A}(m,n)}{\Phi_{\widehat{a}}(1+\vartheta)^{n-m}}\right)^{\vartheta}\times\frac{\mathbb{E}\left[(\widehat{a}(n+1))^{\vartheta}\right]}{\mathcal{M}_{\widehat{a}}(1+\vartheta)}\\&\overset{c}{=}\mathrm{M}_{\widehat{a}}(m,n;\vartheta)\end{aligned}\tag{40}$$

where we use $\mathbb{E}[(\widehat{a}(n+1))^{\vartheta}]/\mathcal{M}_{\widehat{a}}(1+\vartheta)=1$ and the property of i.i.d. can get step c from step b.

The proofs of the service-martingales and arrival-martingales are similar. Based on the assumption that service is i.i.d., for $\vartheta>0$, we have

$$\begin{aligned}&\mathbb{E}[\mathrm{M}_{\widehat{s}}(m,n+1;\vartheta)\mid\widehat{s}(1),\widehat{s}(2),\ldots,\widehat{s}(n)]\\&=\mathbb{E}\left[\left(\frac{\Phi_{\widehat{s}}(1-\vartheta)^{n-m}}{\widehat{S}(m,n)}\right)^{\vartheta}\times\left(\frac{\Phi_{\widehat{s}}(1-\vartheta)}{\widehat{s}(n+1)}\right)^{\vartheta}\right]\\&=\left(\frac{\Phi_{\widehat{s}}(1-\vartheta)^{n-m}}{\widehat{S}(m,n)}\right)^{\vartheta}\mathbb{E}\left[(\widehat{s}(n+1))^{-\vartheta}\right]\mathcal{M}_{\widehat{s}}(1-\vartheta)^{-1}\\&=\mathrm{M}_{\widehat{s}}(m,n;\vartheta)\end{aligned}\tag{41}$$

where $\mathcal{M}_{\widehat{s}}(1-\vartheta)^{-1}\mathbb{E}[(\widehat{s}(n+1))^{-\vartheta}]=1$.

Appendix C
Proof of Theorem 1

Based on (1), we can further obtain

$$\begin{aligned}\Upsilon(n)&=\max\left\{0,\Upsilon(n-1)+c(n)-\sum_{l=1}^{L}h_l(n)\right\}\\&\leq\sup_{0\leq m\leq n}\left\{C(m,n)-\sum_{l=1}^{L}H_l(m,n)\right\}.\end{aligned}\tag{42}$$

Based on (42), Lemmas 1 and 2, the martingale process for energy deficit can be formulated as follows:

$$\begin{aligned}\mathrm{M}_{\Upsilon}(m,n;\alpha)&=\prod_{l=1}^{L}\mu_{h_l}(h_l(n))\mu_c(c(n))\\&\quad\times e^{\alpha\left(\sum_{l=1}^{L}\left((n-m)\Omega_{h_l}-H_l(m,n)\right)+C(m,n)-(n-m)\Omega_c\right)}\end{aligned}\tag{43}$$

where we set $\Omega_c\leq\sum_{l=1}^{L}\Omega_{h_l}$ to satisfy the stability condition of the system. In order to obtain the tightest bounds satisfying the conditions, we further set $\alpha^*=\sup\{\alpha>0:\Omega_c\leq\sum_{l=1}^{L}\Omega_{h_l}\}$. Based on this, (43) can be expressed as

$$\begin{aligned}\mathrm{M}_{\Upsilon}(m,n;\alpha^*)&=\prod_{l=1}^{L}\mu_{h_l}(h_l(n))\mu_c(c(n))\\&\quad\times e^{\alpha^*\left(C(m,n)-\sum_{l=1}^{L}H_l(m,n)\right)}.\end{aligned}\tag{44}$$

By utilizing (42) and (44), the probability bounds for the energy deficit exceeding the battery capacity can be derived as follows:

$$\begin{aligned}&\Pr(\Upsilon(n)>\mathcal{B})\\&\overset{a}{\leq}\Pr\left(\sup_{0\leq m\leq n}\left\{C(m,n)-\sum_{l=1}^{L}H_l(m,n)\right\}>\mathcal{B}\right)\\&\overset{b}{=}\Pr\left(\sup_{0\leq m\leq n}\left\{e^{C(m,n)-\sum_{l=1}^{L}H_l(m,n)}\right\}>e^{\mathcal{B}}\right)\end{aligned}$$

$$\overset{c}{\leq} \Pr\left(\sup_{0\leq m\leq n}\left\{\begin{array}{l}\prod_{l=1}^{L}\mu_{h_l}(h_l(n))\mu_c(c(n))\\ \times\, e^{\alpha^*\left(C(m,n)-\sum_{l=1}^{L}H_l(m,n)\right)}\end{array}\right\} > \Xi e^{\alpha^*\mathcal{B}}\right)$$
$$\overset{d}{\leq} \frac{\prod_{l=1}^{L}\mathbb{E}\left[\mu_{h_l}(h_l(n))\right]\mathbb{E}[\mu_c(c(n))]}{\Xi}e^{-\alpha^*\mathcal{B}} \tag{45}$$

where $\Xi = \min_{c(n)>\sum_{l=1}^{L}h_l(n)}\{\prod_{l=1}^{L}\mu_{h_l}(h_l(n))\mu_c(c(n))\}$. Ξ represents the smallest value of $\prod_{l=1}^{L}\mu_{h_l}(h_l(n))\mu_c(c(n))$ that ensures the EH value of a time slot exceeds the energy harvested value of any time slot in the EH process. The derivation from steps c to d employs the Doob's inequality.

Appendix D
Proof of Theorem 2

Based on (13), Lemmas 3 and 4, we can drive the DVPB as follows:

$$\begin{aligned}&\Pr(W(n) > w)\\ &\overset{a}{\leq} \Pr\left(\sup_{0\leq m\leq n}\left\{\frac{\widehat{A}(m,n)}{\widehat{S}(m,n+w)}\right\}\geq 1\right)\\ &\overset{b}{\leq} \Pr\left(\sup_{0\leq m\leq n}\left\{\left(\frac{\widehat{A}(m,n)}{\Phi_{\widehat{a}}\left(1+\vartheta^{\zeta}\right)^{n-m}}\right.\right.\right.\\ &\qquad\left.\left.\left.\times\frac{\Phi_{\widehat{s}}\left(1-\vartheta^{\zeta}\right)^{n-m+w}}{\widehat{S}(m,n+w)}\right)^{\vartheta^{\zeta}}\right\}\geq \Phi_{\widehat{s}}\left(1-\vartheta^{\zeta}\right)^{\vartheta^{\zeta}w}\right)\\ &\overset{c}{\leq} \Phi_{\widehat{s}}\left(1-\vartheta^{\zeta}\right)^{-\vartheta^{\zeta}w}\end{aligned} \tag{46}$$

where $\vartheta^{\zeta} = \sup\{\vartheta > 0{:}\Phi_{\widehat{a}}(1+\vartheta) \leq \Phi_{\widehat{s}}(1-\vartheta)\}$ is used to obtain the tightest bound and satisfy the stability condition of the queue. The derivation from steps b to c employs the Doobs inequality. The impact of energy storage constraints $(\mathcal{B}, \Psi_b)$ in the hybrid EH-WCS on the arrival and service processes is reflected by parameter ϑ^{ζ}. Based on (4) and Lemma 3, $\Phi_{\widehat{a}}(1+\vartheta) = ((1-\Psi_b)\mathbb{E}[e^{\vartheta r_a(i)}]+\Psi_b)^{1/\vartheta}$ can be obtained. Similarly, with the help of (3) and Lemma 4, we can obtain $\Phi_{\widehat{s}}(1-\vartheta) = ((1-\Psi_b)\mathbb{E}[(1+\gamma(i)\,)^{-[(BT_d\vartheta)/(\ln 2)]}]+\Psi_b)^{-1/\vartheta}$. Additionally, when the hybrid EH process is already known, the mean of $\gamma(i)$ is determined by the energy storage constraints.

With the help of Lemmas 3 and 4, we can construct a backlog martingale in the SNR domain which can be given as follows:

$$\mathrm{M}_Q(m,n;\vartheta) = \left(\frac{\widehat{A}(m,n)}{\Phi_{\widehat{a}}(1+\vartheta)^{n-m}}\times\frac{\Phi_{\widehat{s}}(1-\vartheta)^{n-m}}{\widehat{S}(m,n)}\right)^{\vartheta}. \tag{47}$$

By using (47), we can derive

$$\begin{aligned}&\Pr(Q(n) > \sigma)\\ &\overset{b}{\leq} \Pr\left(\sup_{0\leq m\leq n}\left\{\frac{\widehat{A}(m,n)}{\widehat{S}(m,n)}\right\}\geq e^{\sigma}\right)\\ &\overset{c}{\leq} \Pr\left(\sup_{0\leq m\leq n}\left\{\left(\frac{\widehat{A}(m,n)}{\Phi_{\widehat{a}}\left(1+\vartheta^{\zeta}\right)^{n-m}}\times\frac{\Phi_{\widehat{s}}\left(1-\vartheta^{\zeta}\right)^{n-m}}{\widehat{S}(m,n)}\right)^{\vartheta^{\zeta}}\right\}\geq e^{\vartheta^{\zeta}\sigma}\right)\\ &\overset{d}{\leq} e^{-\vartheta^{\zeta}\sigma}.\end{aligned} \tag{48}$$

References

[1] Z. Fang, J. Wang, Y. Ren, Z. Han, H. V. Poor, and L. Hanzo, "Age of information in energy harvesting aided massive multiple access networks," *IEEE J. Sel. Areas Commun.*, vol. 40, no. 5, pp. 1441–1456, May 2022.

[2] H. Yang, K. Lin, L. Xiao, Y. Zhao, Z. Xiong, and Z. Han, "Energy harvesting UAV-RIS-assisted maritime communications based on deep reinforcement learning against jamming," *IEEE Trans. Wireless Commun.*, vol. 23, no. 8, pp. 9854–9868, Aug. 2024.

[3] X. Lu, P. Wang, D. Niyato, D. I. Kim, and Z. Han, "Wireless networks with RF energy harvesting: A contemporary survey," *IEEE Commun. Surveys Tuts.*, vol. 17, no. 2, pp. 757–789, 2nd Quart., 2015.

[4] Z. Ni, Z. Zhang, N. C. Luong, D. Niyato, D. I. Kim, and S. Feng, "Joint client scheduling and quantization optimization in energy harvesting-enabled federated learning networks," *IEEE Trans. Wireless Commun.*, vol. 23, no. 8, pp. 9566–9582, Aug. 2024.

[5] D. Niyato, E. Hossain, and A. Fallahi, "Sleep and wakeup strategies in solar-powered wireless sensor/mesh networks: Performance analysis and optimization," *IEEE Trans. Mob. Comput.*, vol. 6, no. 2, pp. 221–236, Nov. 2007.

[6] S. Hu, X. Chen, W. Ni, X. Wang, and E. Hossain, "Modeling and analysis of energy harvesting and smart grid-powered wireless communication networks: A contemporary survey," *IEEE Trans. Green Commun. Netw.*, vol. 4, no. 2, pp. 461–496, Jun. 2020.

[7] D. Wang, W. Wang, Z. Han, and Z. Zhang, "Delay optimal random access with heterogeneous device capabilities in energy harvesting networks using mean field game," *IEEE Trans. Commun.*, vol. 20, no. 9, pp. 5543–5557, Sep. 2021.

[8] K. Zheng, J. Wang, X. Liu, X.-W. Yao, Y. Xu, and J. Liu, "A hybrid communication scheme for throughput maximization in backscatter-aided energy harvesting cognitive radio networks," *IEEE Internet Things J.*, vol. 10, no. 18, pp. 16194–16208, Sep. 2023.

[9] S. Yang, J. Tan, T. Lei, and B. Linares-Barranco, "Smart traffic navigation system for fault-tolerant edge computing of Internet of Vehicle in intelligent transportation gateway," *IEEE Trans. Intell. Transp. Syst.*, vol. 24, no. 11, pp. 13011–13022, Nov. 2023.

[10] O. A. Saraereh, A. Alsaraira, I. Khan, and B. J. Choi, "A hybrid energy harvesting design for on-body Internet-of-Things (IoT) networks," *Sensors*, vol. 20, no. 2, p. 407, Jan. 2020.

[11] D. Altinel and G. K. Kurt, "Modeling of hybrid energy harvesting communication systems," *IEEE Trans. Green Commun. Netw.*, vol. 3, no. 2, pp. 523–534, Jun. 2019.

[12] A. Celik, A. Alsharoa, and A. E. Kamal, "Hybrid energy harvesting-based cooperative spectrum sensing and access in heterogeneous cognitive radio networks," *IEEE Trans. Cogn. Commun. Netw.*, vol. 3, no. 1, pp. 37–48, Mar. 2017.

[13] C. Fu et al., "Throughput maximization in wireless communication systems powered by hybrid energy harvesting," *IEEE Trans. Comput.-Aided Design Integr. Circuits Syst.*, vol. 41, no. 11, pp. 3981–3992, Nov. 2022.

[14] Y. Zhang et al., "Power optimization for massive MIMO systems with hybrid energy harvesting transmitter," *IEEE Trans. Veh. Technol.*, vol. 67, no. 10, pp. 10039–10043, Oct. 2018.

[15] D. W. K. Ng, E. S. Lo, and R. Schober, "Energy-efficient resource allocation in OFDMA systems with hybrid energy harvesting base station," *IEEE Trans. Wireless Commun.*, vol. 12, no. 7, pp. 3412–3427, Jul. 2013.

[16] M. Calvo-Fullana, C. Antón-Haro, J. Matamoros, and A. Ribeiro, "Stochastic routing and scheduling policies for energy harvesting communication networks," *IEEE Trans. Signal Process.*, vol. 66, no. 13, pp. 3363–3376, Jul. 2018.

[17] L. Pang et al., "Energy-efficient resource optimization for hybrid energy harvesting massive MIMO systems," *IEEE Syst. J.*, vol. 16, no. 1, pp. 1616–1626, Mar. 2022.

[18] H. Al-Zubaidy, V. Fodor, G. Dán, and M. Flierl, "Reliable video streaming with strict playout deadline in multihop wireless networks," *IEEE Trans. Multimedia*, vol. 19, no. 10, pp. 2238–2251, Oct. 2017.

[19] R. Liptser and A. N. Shiryayev, *Theory of Martingales*, vol. 49. Berlin, Germany: Springer, 2012.

[20] Z. Wang, B. Lin, Q. Ye, Y. Fang, and X. Han, "Joint computation offloading and resource allocation for maritime MEC with energy harvesting," *IEEE Internet Things J.*, vol. 11, no. 11, pp. 19898–19913, Jun. 2024.

[21] Z. Li, Y. Gao, P. Li, B. A. Salihu, L. Sang, and D. Yang, "Throughput analysis of an energy harvesting multichannel system under delay and energy storage constraints," *IEEE Trans. Veh. Technol.*, vol. 66, no. 9, pp. 7818–7832, Sep. 2017.

[22] Z. Li, Y. Jiang, Y. Gao, L. Sang, and D. Yang, "On buffer-constrained throughput of a wireless-powered communication system," *IEEE J. Sel. Areas Commun.*, vol. 37, no. 2, pp. 283–297, Sep. 2019.

[23] B. Varan and A. Yener, "Delay constrained energy harvesting networks with limited energy and data storage," *IEEE J. Sel. Areas Commun.*, vol. 34, no. 5, pp. 1550–1564, May 2016.

[24] H. Al-Zubaidy, J. Liebeherr, and A. Burchard, "Network-layer performance analysis of multihop fading channels," *IEEE/ACM Trans. Netw.*, vol. 24, no. 1, pp. 204–217, Feb. 2016.

[25] Y. Zhou, L. Feng, X. Jiang, W. Li, and F. Zhou, "Predictable wireless networked scheduling for bridging hybrid time-sensitive and real-time services," *IEEE Trans. Commun.*, vol. 72, no. 6, pp. 3664–3680, Jun. 2024.

[26] C. Xiao, J. Zeng, W. Ni, R. P. Liu, X. Su, and J. Wang, "Delay guarantee and effective capacity of downlink NOMA fading channels," *IEEE J. Sel. Topics Signal Process.*, vol. 13, no. 3, pp. 508–523, Jun. 2019.

[27] J. Zeng, C. Xiao, T. Wu, W. Ni, R. P. Liu, and Y. J. Guo, "Uplink non-orthogonal multiple access with statistical delay requirement: Effective capacity, power allocation, and α fairness," *IEEE Trans. Wireless Commun.*, vol. 22, no. 2, pp. 1298–1313, Feb. 2023.

[28] Y. Chen, H. Lu, L. Qin, C. Zhang, and C. W. Chen, "Statistical QoS provisioning analysis and performance optimization in xURLLC-enabled massive MU-MIMO networks: A stochastic network calculus perspective," *IEEE Trans. Wireless Commun.*, vol. 23, no. 7, pp. 8044–8058, Jul. 2024.

[29] W. Miao, G. Min, Z. Yu, and X. Zhang, "Performance analytical Modelling of mobile edge computing for mobile vehicular applications: A worst-case perspective," *IEEE Trans. Mobile Comput.*, vol. 23, no. 9, pp. 8951–8964, Sep. 2024.

[30] M. Mei, M. Yao, Q. Yang, J. Wang, Z. Jing, and T. Q. Quek, "Network-layer delay provisioning for integrated sensing and communication UAV networks under transient antenna misalignment," *IEEE Trans. Wireless Commun.*, early access, May 14, 2024, doi: 10.1109/TWC.2024.3397827.

[31] H. Peng, C.-C. Hsia, Z. Han, and L.-C. Wang, "A generalized delay and backlog analysis for multiplexing URLLC and eMBB: Reconfigurable intelligent surfaces or decode-and-forward?" *IEEE Trans. Wireless Commun.*, vol. 23, no. 5, pp. 4049–4068, May 2024.

[32] T. Liu, H. Zhou, J. Li, F. Shu, and Z. Han, "Uplink and downlink decoupled 5G/B5G vehicular networks: A federated learning assisted client selection method," *IEEE Trans. Veh. Technol.*, vol. 72, no. 2, pp. 2280–2292, Feb. 2023.

[33] B. Picano and R. Fantacci, "A combined stochastic network calculus and matching theory approach for computational offloading in a heterogenous MEC environment," *IEEE Trans. Netw. Serv. Manag.*, vol. 21, no. 2, pp. 1958–1968, Apr. 2024.

[34] W. Yang, X. Chi, L. Zhao, and R. Qi, "Predictive two-timescale resource allocation for VoD services in fast moving scenarios," *IEEE Trans. Veh. Technol.*, vol. 70, no. 10, pp. 10002–10017, Oct. 2021.

[35] H. Yan, X. Chi, W. Yang, and Z. Han, "End-to-end delay analysis for multi-hop wireless links based on martingale theory," *IEEE Trans. Veh. Technol.*, early access, Apr. 16, 2024, doi: 10.1109/TVT.2024.3389704.

[36] H. Rezaee, K. Zhang, T. Parisini, and M. M. Polycarpou, "Cooperative adaptive cruise control in the presence of communication and radar stochastic data loss," *IEEE Trans. Intell. Transp. Syst.*, vol. 25, no. 6, pp. 4964–4976, Jun. 2024.

[37] R. McEliece and W. Stark, "Channels with block interference," *IEEE Trans. Inf. Theory*, vol. 30, no. 1, pp. 44–53, Jan. 1984.

[38] R. Rajesh, V. Sharma, and P. Viswanath, "Capacity of Gaussian channels with energy harvesting and processing cost," *IEEE Trans. Inf. Theory*, vol. 60, no. 5, pp. 2563–2575, May 2014.

[39] Y. A. Brychkov, O. I. Marichev, and N. V. Savischenko, *Handbook of Mellin Transforms*. Boca Raton, FL, USA Chapman and Hall, 2018.

[40] Y. Mao, G. Yu, and C. Zhong, "Energy consumption analysis of energy harvesting systems with power grid," *IEEE Wireless Commun. Lett.*, vol. 2, no. 6, pp. 611–614, Dec. 2013.

[41] S. Zhang, A. Seyedi, and B. Sikdar, "An analytical approach to the design of energy harvesting wireless sensor nodes," *IEEE Trans. Wireless Commun.*, vol. 12, no. 8, pp. 4010–4024, Aug. 2013.

[42] A. Mehemed and W. Hamouda, "AF cooperative CDMA outage probability analysis in Nakagami-*m* fading channels," *IEEE Trans. Veh. Technol.*, vol. 62, no. 3, pp. 1169–1176, Mar. 2013.

[43] I. S. Gradshteyn and I. M. Ryzhik, *Table of Integrals, Series, and Products*. New York, NY, USA: Academic, 2007.